Review

A Topological Approach Unveils System Invariances and Broken Symmetries in the Brain

Arturo Tozzi[1]★ and James F. Peters[2]

[1]Center for Nonlinear Science, University of North Texas, Denton, Texas
[2]Department of Electrical and Computer Engineering, University of Manitoba, Winnipeg, Manitoba, Canada

Symmetries are widespread invariances underscoring countless systems, including the brain. A symmetry break occurs when the symmetry is present at one level of observation but is hidden at another level. In such a general framework, a concept from algebraic topology, namely, the Borsuk-Ulam theorem (BUT), comes into play and sheds new light on the general mechanisms of nervous symmetries. The BUT tells us that we can find, on an n-dimensional sphere, a pair of opposite points that have the same encoding on an $n - 1$ sphere. This mapping makes it possible to describe both antipodal points with a single real-valued vector on a lower dimensional sphere. Here we argue that this topological approach is useful for the evaluation of hidden nervous symmetries. This means that symmetries can be found when evaluating the brain in a proper dimension, although they disappear (are hidden or broken) when we evaluate the same brain only one dimension lower. In conclusion, we provide a topological methodology for the evaluation of the most general features of brain activity, i.e., the symmetries, cast in a physical/biological fashion that has the potential to be operationalized.   © 2016 Wiley Periodicals, Inc.

Key words: hidden symmetry; Central nervous system; Borsuk-Ulam theorem; invariance

Symmetry is a type of invariance occurring when a structured object does not change under a set of transformations (Weyl, 1982). Symmetries hold the key for understanding many of nature's intimate secrets because they are the most general feature of countless types of systems. Huge swathes of mathematics, physics, and biology, including the brain, can be explained in terms of the underlying invariance of the structures under investigation. In physics, symmetries can be "broken." Symmetry breaking consists of sudden change in the set of available states; the whole phase space is partitioned into nonoverlapping regions (Roldàn et al., 2014) so that small fluctuations acting on a system cross a critical point and decide which branch of a bifurcation is taken. In particular, in spontaneous symmetry breaking (SSB), the underlying laws are invariant under a symmetry transformation, but the system as a whole changes. SSB is a process that allows a system cast in a symmetrical state to end up in an asymmetrical one. SSB describes systems in which the equations of motion or the Lagrangian obey certain invariances, but the lowest energy solutions do not exhibit them. "Hidden" is perhaps a better term than "broken" because the symmetry is always there in such equations (Higgs, 1964). In the case of finite systems with metastable states, the confinement is not strict; the system can "jump" from one region to another (Roldàn et al., 2014). With respect to the brain, its activity is an example of an open system, partially stochastic resulting from intrinsic fluctuations but containing islands at the edge of the chaos, that maintains homeostasis or allostasis in the face of environmental fluctuations (Friston, 2010). The

SIGNIFICANCE

This Review provides a theoretical/methodological framework based on simple topological concepts that make possible the evaluation of brain parameters in terms of their dimensionality, symmetries, and symmetry breaking. The brain functional and anatomical organization may be better assessed if one considers how certain hidden symmetries, essential for shaping brain gradients and activity, may appear only under the lens of higher dimensional neural representations. We explain the computational and thermodynamic interest of such topologies and offer concrete examples of their possible applications to neuroscience. This Review emphasizes the role of a rigorous mathematical apparatus in unifying and operationalizing deep multidisciplinary theoretical questions.

★Correspondence to: Arturo Tozzi, Center for Nonlinear Science, University of North Texas, 1155 Union Circle No. 311427, Denton, TX 76203-5017. E-mail: tozziarturo@libero.it
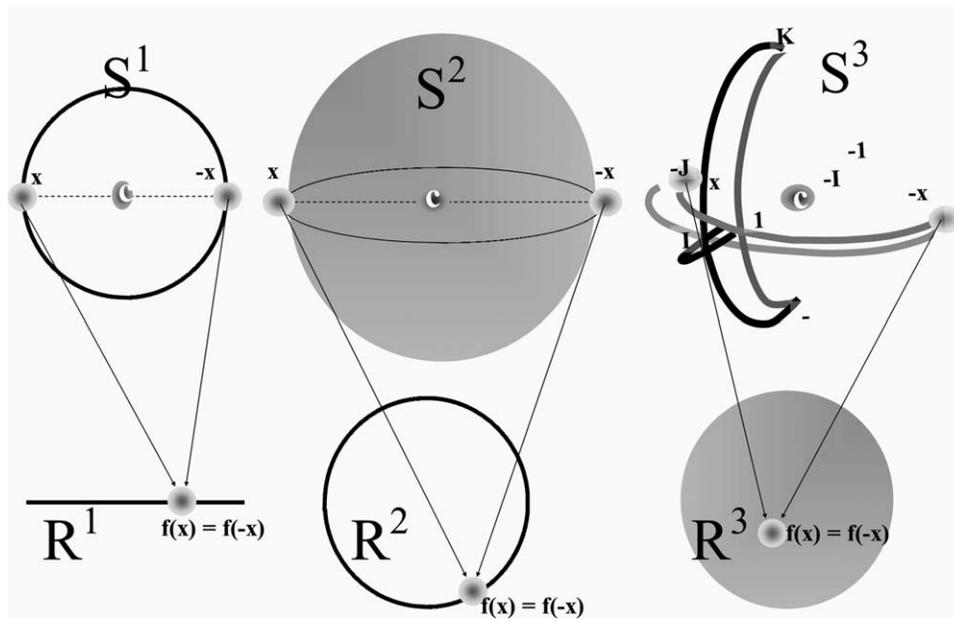
Fig. 1. The BUT for different values of S^n. Two antipodal points in S^n project to a single point in R^n and vice versa. Remember that every S^n is embedded in an $n + 1$-ball; thus, every S^n is one dimension higher than the corresponding R^n.

brain retains the characteristics of a complex, nonlinear system with nonequilibrium dynamics (Fraiman and Chialvo, 2012), equipped with random walks (Afraimovich et al., 2013). It operates at the edge of chaos (Tognoli and Kelso, 2014) and lives near a metastable state of second-order phase transition between micro- and macrolevels (Beggs and Timme, 2012), characterized by infinite correlation length, countless dimensions, slight nonergodicity, attractors (Deco and Jirsa, 2012), and universal power laws, evidenced by the presence of spontaneous neuronal avalanches (De Arcangelis and Herrmann, 2010).

In such a multifaceted framework, the Borsuk-Ulam theorem (BUT) is useful. This theorem tells us that, if a sphere is mapped continuously into a plane set, there is at least one pair of antipodal points having the same image; that is, they are mapped in the same point of the plane (Beyer and Zardecki, 2004). Here, we show that brain symmetries hidden at a lower level are detectable at a higher level of analysis and vice versa. In other words, a symmetry break occurs when the symmetry is present at one level of observation but hidden at another level.

This theoretical Review comprises six sections. In the first section, we show how brain symmetries can be studied in a topological fashion, i.e., in terms of antipodal points on a hypersphere. If we enclose symmetries equipped with antipodal self-similar points into the abstract spaces of n–spheres, they can be evaluated in the guise of projections on S^{n-1}, where they stand for the broken symmetry. The second through fourth sections explain how we are allowed to generalize the BUT to the study of all the types of brain symmetries. In particular,

section 2 illustrates how the symmetries are not required to be framed only as antipodal points on spatial n-spheres, as stated by the "classical" BUT, but can also be embedded in every kind of n-sphere equipped with other types of dimensions. Section 3 further expands the possible use of the BUT in the study of symmetries by showing that they can also occur between two nonantipodal points embedded in an n-sphere. Section 4 is devoted to extending the concept of symmetries from systems formed by convex spheres to the concave, hyperbolic manifolds that are thought to be the natural frame of brain activity. The fifth section lists the best candidates that may represent a symmetry (and Lagrangian) to formulate a BUT theory for the nervous system. Throughout sections 1–5, we also provide concrete examples of applications of symmetry and symmetry breaking in neuroscience to show that our theory can be operationalized in the study of brain anatomy, function, and dynamics. The final section describes the methodological advantages of the topological approach to nervous symmetries.

NERVOUS SYMMETRIES AS ANTIPODAL POINTS ON AN N-SPHERE

The BUT is a remarkable finding by K. Borsuk (1933) about Euclidean n-spheres and antipodal points. It states that every continuous map, $f:S^n \rightarrow R^n$, must identify a pair of antipodal points (on S^n; Dodson and Parker, 1997; Fig. 1).

The sphere S^n maps to R^n, which is an n-dimensional Euclidean space. Another less technical definition is, if a sphere is mapped continuously into a plane set, there is at least one pair of antipodal points having the

same image; that is, they are mapped in the same point of the plane (Beyer and Zardecki, 2004). For other definitions of the BUT and its countless proofs, see Matoušek (2003) and Peters (2016).

The notation S^n denotes an n-sphere, which is a generalization of the circle (Weeks, 2002). An n-sphere is an n-dimensional structure embedded in an $n + 1$ space. For example, a 1-sphere (S^1) is the one-dimensional circumference surrounding a two-dimensional disk, whereas a 2-sphere (S^2) is the two-dimensional surface of a three-dimensional ball (a beach ball is a good example). An n-hypersphere (briefly, n-sphere or S^n) is formed by points that are constant distances from the origin in $n + 1$ dimensions (Marsaglia, 1972). For example, a 3-sphere (also called a *glome*) of radius r (where r may be any positive real number) is defined as the set of points in four-dimensional Euclidean space at distance r from some fixed center point c (which may be any point in the four-dimensional space; Moura and Henderson, 1996). A 3-sphere is a simply connected three-dimensional manifold of constant, positive curvature that is enclosed in a Euclidean four-dimensional space called a "4-ball." A 3-sphere is thus the surface or boundary of a four-dimensional ball, and a four-dimensional ball is the interior of a 3-sphere in the same way that a bottle of water is made of a glass surface and a liquid content.

Points on S^n are antipodal, provided that they are diametrically opposite (Weisstein, 2015). Examples of antipodal points are the endpoints of a line segment, the opposite points along the circumference of a circle, or the poles of a sphere. Furthermore, every continuous function from an n-sphere S^n into Euclidean n-space R^n maps some pair of antipodal points of S^n to the same point of R^n. For example, if we use the mapping $f:S^3 \to R^3$, then $f(x)$ in R^3 is only a signal value (a real number associated with x in S^3) and $f(x) = f(-x)$ in R^3. Furthermore, when $g:S^2 \to R^2$, the $g(x)$ in R^2 is a vector in R^2 that describes the x embedded in S^2. In other words, a point embedded in an R^n manifold is projected to two opposite points on an S^{n+1}-sphere and vice versa. The next sections highlight the versatility of the three main ingredients of the BUT, the antipodal points with matching description, the n-sphere, and the possibility to map into an $n - 1$ sphere.

DESCRIPTION OF A SIGNAL THROUGH THE BUT

In terms of activity, a feature vector $x \in R^n$ models the description of a signal. To elucidate the picture in the application of the BUT in signal analysis, we view the surface of a manifold as an n-sphere and the feature space for signals as finite Euclidean topological spaces. The BUT tells us that for description $f(x)$ for a signal x, we can expect to find an antipodal feature vector $f(-x)$ that describes a signal on the opposite (antipodal) side of the manifold S^n. Thus, the pair of antipodal signals has matching descriptions on S^n.

Let X denote a nonempty set of points on the surface of the manifold. A topological structure on X (called a "topological space") is a structure given by a set of subsets τ of X, having the following properties: Str1, every union of sets in τ is a set in τ; Str2, every finite intersection of sets in τ is a set in τ.

The pair (X,t) is called a topological space. Usually, X by itself is called a topological space, provided X has a topology τ on it. Let (X,Y) be topological spaces. Recall that a function or map $f:X \to Y$ on a set X to a set Y is a subset $X \times Y$ so that for each $x \in X$ there is a unique $y \in Y$ such that $(x, y) \in f$ [usually written $y = f(x)$]. The mapping f is defined by a rule that tells us how to find $f(x)$. For a good introduction to mappings, see Willard (1970).

SHAPES AND HOMOTOPIES

A mapping $f:X \to Y$ is continuous, provided that, when $A \subset Y$ is open, then the inverse $f^{-1}(A) \subset X$ is also open. For more about this, see Krantz (2009). In this view of continuous mappings from the signal topological space X on the manifold's surface to the signal feature space R^n, we can consider not only one signal feature vector $x \in R^n$ but also mappings from X to a set of signal feature vectors $f(X)$. This expanded view of signals has interest because every connected set of feature vectors $f(X)$ has a shape. The significance of this is that signal shapes can be compared.

A consideration of $f(X)$ set of signal descriptions for a region (X) instead of $f(X)$ (description of a single signal x) leads to a region-based view of signals. This region-based view of the manifold arises naturally in terms of a comparison of shapes produced by different mappings from X (object space) to the feature space R^n. An interest in continuous mappings from object spaces to feature spaces leads to homotopy theory and the study of shapes.

Let $f,g:X \to Y$ be continuous mappings from X to Y. The continuous map $H:X \times [0,1] \to Y$ is defined by $H(x,0) = f(x)$, $H(x,1) = g(x)$, for every $x \in X$. The mapping H is a homotopy, provided that there is a continuous transformation (called a "deformation") from f to g. The continuous maps f,g are called "homotopic maps," provided that $f(X)$ continuously deforms into $g(X)$ [denoted by $f(X) \to g(X)$]. The sets of points $f(X)$, $g(X)$ are called "shapes." For more about this, see Manetti (2015) and Cohen (1973).

It was Borsuk who first associated the geometric notion of shape and homotopies. There are natural ties between Borsuk's result for antipodes and mappings called "homotopies." The early work on n-spheres and antipodal points eventually led Borsuk to the study of retraction and homotopic mappings (Borsuk, 1958–1959, 1969; Borsuk and Gmurczyk, 1980). This leads into the geometry of shapes and shapes of space (Collins, 2004). A pair of connected planar subsets in Euclidean space R^2 have equivalent shapes, provided that the planar sets have the same number of holes (22). For example, the letters e, O, P and the numerals 6, 9 belong to the same equivalence class of single-hole shapes. In terms of signals, it means that the connected graph for $f(X)$ with, for example, an e

shape can be deformed into the 9 shape. This suggests yet another useful application of Borsuk's view of the transformation of a shape into another, in terms of signal analysis. Sets of signals will have not only similar descriptions but also dynamic character. Moreover, the deformation of one signal shape into another occurs when they are descriptively near (Peters, 2014).

In sum, the concept of antipodal points can be generalized to countless types of system signals. The two antipodal points can indeed be used for the description not only of simple topological points but also of more complicated structures, such as shapes of space (spatial patterns), shapes of time (temporal patterns), thermodynamical parameters, movements, trajectories, and general symmetries (Peters, 2014).

If we evaluate simply CNS activity instead of signals, the BUT leads naturally to the possibility of a region-based, not simply point-based, brain geometry, with many applications. A brain region can indeed have features such as area, diameter, average signal value, trajectories, and so on (Peters, 2016). We are thus allowed to describe brain symmetries as antipodal points on an n-sphere. If we map the two points on an $n-1$-sphere, we obtain a single point. Here, the symmetry is hidden; i.e., it is not visible in dimension $n-1$. A spontaneous symmetry breaking occurs when a symmetry is not a property of the individual states of a system but is a property of the mathematical structure that models the physical system. This is the case with the antipodal points on an n-sphere that can be mapped to the same signal value. To restore the apparently broken symmetry, we are required to evaluate only the single point in a dimension higher, where the two antipodal points will appear and the symmetry, hidden in the lower dimension, will be refurbished. In conclusion, if we enclose brain symmetries, equipped with antipodal self-similar points, into the abstract spaces of n-spheres, the former can be evaluated in the guise of projections on S^{n-1}. The two antipodal points standing for symmetries are assessed at one level of observation, whereas the single point standing for the broken symmetry is assessed at a lower level of observation.

AN EXAMPLE: INTERPRETATION OF A TESSELLATION OF AN FMRI

Here we specify the nature of the observables and the mapping of signals into the feature space used for the analysis of brain activity, and we show an application to available data sets to explain why our proposed approach offers an advance over the current set of tools. To do this, we include an application showing a graphic analysis of a brain fMRI (a so-called Delaunay tessellation) to understand better some aspects of brain computation and/or function viewed in the context of the predictions of the BUT.

We must first build a Delaunay tessellation. Each key point signal is chosen because of its feature values, which sharply contrast with its neighboring signal values. The Delaunay triangulation connects with a pair of near-

est key points with a straight edge, resulting in a collection of triangles covering an image (Edelsbrunner, 2014). In its simplest form, a key point is chosen based on dominant color intensity and pixel gradient. That is, the gradient orientation of a pixel is the angle of the tangent to the pixel. A pixel gradient dominates, provided that the gradient differs sharply from its neighbors. Consider Figure 2, which contains tessellations of four fMRI images from Fox et al. (2015). The triangle vertices in the four Delaunay triangulation fMRI images are dominant (key point) brain signals in a collection of 1-sphere surface values. The upper half of Figure 2 contains a Delaunay mesh in situ (Fig. 2A) and a Delaunay mesh projected onto a 1-sphere (Fig. 2B). The lower half of Figure 2 contains the Delaunay mesh plot by itself (Fig. 2C) and the Delaunay mesh projected onto a 2-sphere by itself (Frank and Hart, 2010; Fig. 2D). If we look at this key point-based Delaunay mesh in Figure 2, we see that 1) key points associated with brain signals with high intensity and gradient orientation differ from those of neighboring fMRI pixels; 2) the Delaunay mesh connects each pair of fMRI key point pixels nearest each other; 3) the Delaunay mesh includes connections between key points among the pairs of fMRI images; 4) the connections among the four fMRI images represent mappings predicted by the BUT; i.e., at least one pair of fMRI key points is connected to a key point on another image; 5) fMRI pixel intensity and gradient orientation of a fMRI key point constitute a feature vector in R^n (Fig. 2D).

In sum, we are able to predict the occurrence of antipodal points on different fMRI images by knowing the activated points on only one of them. In effect, this means that we can know in advance which brain areas are activated at the same time. Novel patterns of simultaneous (or sequential) activities of different (smaller or larger) brain zones could be discovered and transferred to a lower dimension R^n manifold.

SYMMETRIES CAN BE EMBEDDED IN DIFFERENT KINDS OF N-SPHERES

The BUT can be generalized to all types of brain symmetries. Although the BUT had originally been described just in the case of n being a natural number that expresses a spatial dimension, nevertheless the value of n in the brain, S^n, can also stand for a fractional or an irrational number. The n exponent is not required either to be a natural number or to be embedded in a spatial dimension. We are allowed to modify the BUT's exponent on an n-sphere and to change a natural number into a rational or irrational one to describe n in a brain symmetric system equipped with two antipodal points. We are allowed indeed, if we take into account a BUT on d-spheres with Hausdorff dimension d, which is a fraction between 0 and 1 and is an expression of the fractal dimension.

We used the following terminology. Metric space: let X be a metric space with the metric $\mu_d(X)$ defined on it. This means that $\mu_d(X) \geq 0$ and that μ_d has the usual symmetry and triangle inequality properties for all subsets
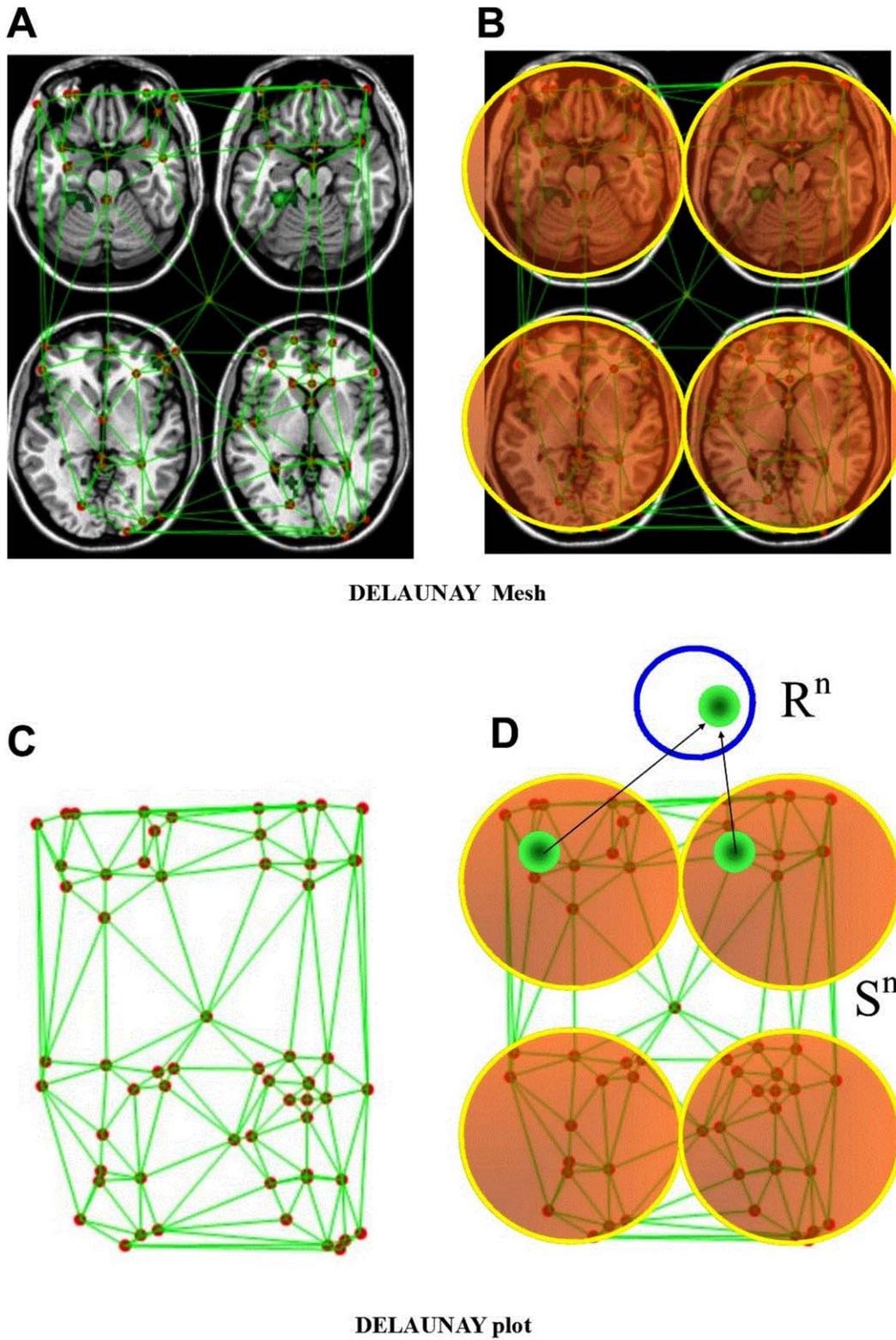
Fig. 2. Meta-analytic activations associated with mind wandering and related spontaneous thought processes throughout the entire brain. Horizontal slices are presented with 3-mm skip (modified from Fox et al., 2015). **A,C** show Delaunay tessellation; **B,D** show the same images embedded in S^n spheres, according to the BUT dictates. See article text for further details.

of X. Hausdorff measure: let d be either 0 or a positive real number in R_0^+. The Hausdorff measure $\mu_d(X)$ equals a real number for each number d in $X = R^d$. Hausdorff dimension (informal): the threshold value of d denoted by $\dim_H(X)$ is the Hausdorff dimension of X, provided that $\mu_d(X) = 0$ if $d > \dim_H(X)$ and $\mu_d(X) = \infty$ if $d < \dim_H(X)$.

Lemma

Schleicher boundedness lemma. Let d be any real number in R_0^+ and let Y be a metric space. If $X \subset Y$, then $\dim_H(X) \leq \dim_H(Y)$.

Proof: immediate from the definition of the Hausdorff dimension of a nonempty set. Assume that X is a nonempty subset (inner sphere) of an n-sphere and has the same center as S^n with the Hausdorff measure $\mu_d(X)$ defined on it, and assume that $\mu_d(X)$ satisfies the Schleicher lemma conditions. The inner sphere S^d of an n-sphere S^n can be any subsphere in S^n, including S^n itself. Then, the inner sphere S^d has dimension $d = \dim_H(X)$, $d \leq n$. In addition, assume that R^d is a d-dimensional space that is a subset of the n-dimensional Euclidean space R^n, $d < n$. This gives us a new form of the BUT (Borsuk, 1933).

Theorem

Hausdorff–Borsuk–Ulam theorem. Let S^d with Hausdoff dimension d be an inner sphere of an n-sphere and let $f\colon S^d \to R^d$ be a continuous map. There exists a pair of antipodal points on S^d that are mapped to the same point in R^d.

Proof. A direct proof that this theorem is symmetric with the proof of the BUT is given by Su (1997), given that we assume that S^d is an inner sphere of S^n symmetric around the center of S^n and, from the Schleicher boundedness lemma, $\dim_H(S^d) \leq \dim_H(S^n)$.

Summary. The BUT can be used not only for the description of spatial dimensions equipped with natural numbers but also for the description of antipodal points on brain d-spheres equipped with (fractal) Hausdorff dimension d. The same mechanism also stands for other kinds of n-spheres' dimensions other than fractals. It allows us to use the n parameter as a versatile tool for the description of CNS symmetries. The n exponent of S^n can be cast as an integer, a rational number (the above-mentioned case of self-similarity and fractal dimensions; see also paragraph 5), or an irrational number (in case we want to evaluate nonlinear, chaotic brain as embedded in a Feigenbaum constant's dimension; see example 2 below; Smith, 2013). The n exponent could stand for completely different parameters; for example, we might regard brain circadian rhythms as embedded in a sphere in which n stands for the time and not for a spatial dimension. In such a vein, we may also regard the temporal symmetries in EEG as antipodal points characterized by similarities in time occurrence and not in shape.
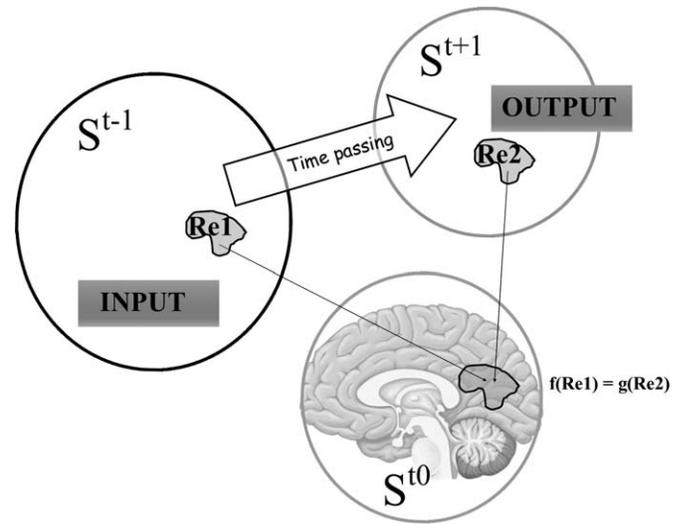

Fig. 3. A system formed by n-spheres in which n stands for a time dimension. The antipodal points $\mathrm{Re}1$ and $\mathrm{Re}2$ are located on a sphere equipped with a dimension of time $t - 1$ (the past) and with a dimension of time $t + 1$ (the future), respectively. The brain, equipped with time $t0$, stands for the present.

Example 1: From Stimuli to Brain Responses

The brain, in a topological framework, might stand for a system formed by two variables connected in a way such that when one changes the other changes. The initial state occurs before the variation, and the final state occurs afterward (Fig. 3). The changes can be either real or merely possible. The final state depends on two settings, the initial state of the system and the external factors acting on the system. Note that, in this case, in touch with dictates of the BUT variant, the system is formed by n-spheres equipped with time but not spatial dimensions.

Example 2: Phase Transitions and Nonlinear Dynamics in the Brain

The brain is believed to be an open system that maintains a nonequilibrium steady state (i.e., homoeostasis or allostasis) in the face of continuous environmental fluctuations (Van de Ville et al., 2010; Friston et al., 2014). It displays complex, nonlinear dynamic features and is equipped with a large number of interacting and interdependent components with random walks (Perkins et al., 2014), circular causality (Fraiman and Chialvo, 2013), and self-organized criticality (Bak et al., 1987). The brain is also said to operate at the edge of chaos (a regime characterized by dependence from initial conditions, positive Lyapunov exponents, and attractors) and tends to live near a metastable state of second-order phase transition (Afrahimovich et al., 2013; De Arcangelis et al., 2006). Sequential, hierarchical self-organization on an increasing scale leads to passage beyond reversibility in space as well as in time and to the emergence of novel features and properties at each level (Beggs and Timme, 2012; Taylor and Ehrenreigh, 2014). In this complex framework, the

BUT variant is able to elucidate (at least some of) the dynamics underlying the nonlinear brain. We must first introduce the "logistic map," which is a one-dimensional nonlinear difference equation widely used to study equations in the field of dynamic systems theory. For example, take into account the coupled equations (Richardson et al., 2014)

$$X_{(t+1)} = r_1 x_{(t)}\left(1 - x_{1(t)}\right) + \alpha r_2 x_{2(t)} \frac{\left(1 - x_{2(t)}\right)}{1+\alpha},$$

$$X_{2(t+1)} = r_2 x_{2(t)}\left(1 - x_{2(t)}\right) + \alpha_1 r_1 x_{1(t)} \frac{\left(1 - x_{2(t)}\right)}{1+\alpha},$$

where x is a generic variable representing some observable behavior, r is a fixed behavioral parameter (the phase parameter), and t equals time from step 0 to step n. A logistic map may be simply plotted and visualized on a one-parameter bifurcation diagram as a function of the scaled parameter r (Fig. 4A). At the edge of criticality, a so-called Hopf bifurcation occurs. In general, every chaotic system that corresponds to a one-dimensional map with a single quadratic maximum will bifurcate at the same rate (Alligood et al., 1996); the limiting ratio of each bifurcation interval to the next between every period doubling is 4.6692 .... . This value is called the first universal "Feigenbaum constant" (Smith, 2013); note that that such a constant is a transcendental number (Jordan and Smith, 2007).

Through our BUT variant, we achieve an n-sphere with an n-exponent corresponding to the Feigenbaum number. The next step is to locate the n-sphere on the above-mentioned logistic map to embed the topological antipodal points into the bifurcation diagram (Fig. 4A). After having achieved two antipodal points for every bifurcation, we are allowed to map them in the concentric layers of another n-sphere (Fig. 4B). We obtain a novel topological n-sphere that summarizes the whole behavior of a nonlinear system in phase transition, such as the brain. Note that the center of the sphere stands for a completely linear system, whereas, when we move along the circumference toward the sphere surface, we achieve antipodal points representing a progressively more chaotic system. In such a vein, knowledge of just the single central point and the first Feigenbaum constant leads to predictions about the temporal development of the phenomena occurring in the brain at the edge of chaos.

SYMMETRIES ARE NOT REQUIRED TO BE ANTIPODAL POINTS ON N-SPHERES

The applications of the BUT can be generalized not just for the evaluation of brain symmetries as antipodal points on an n-sphere but also as nonantipodal points. Indeed, a theorem derived from the BUT, the region-based version of the BUT (Re-BUT), is as follows. Let 2^{Sn} be a family of regions on an n-sphere. A region can have features such as area, diameter, average signal value, and so on.
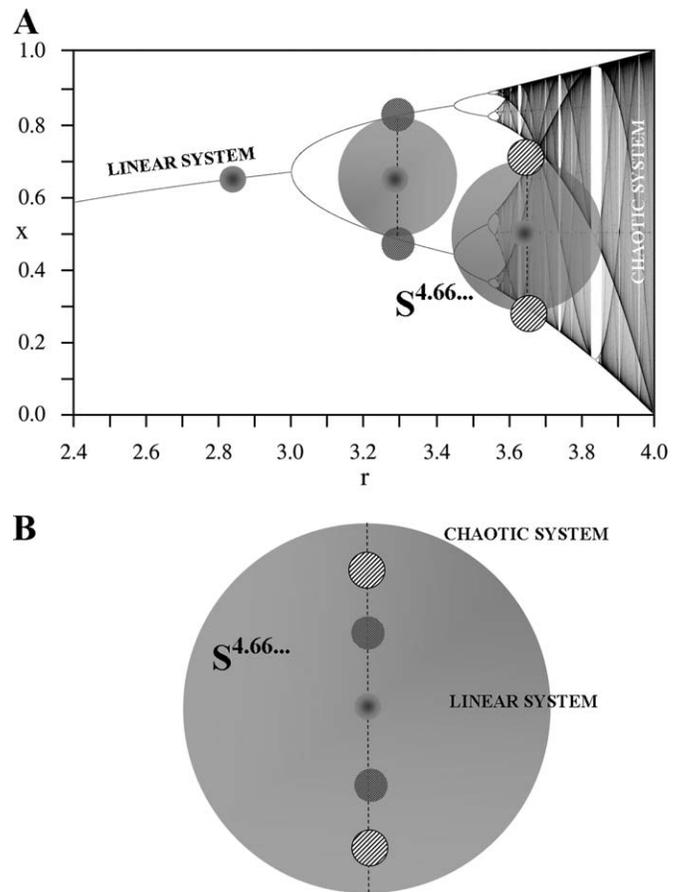

Fig. 4. **A:** Bifurcation diagram of a logistic map's nonlinear dynamic equation. The x axis displays the phase parameter. At the first Hopf bifurcation, the exponent n of the n-sphere corresponds to the first Feigenbaum constant. The same operation can be repeated at each of the following bifurcations; only the first and the second ones are displayed in the figure. Each sphere is equipped with two antipodal points that intersect the curves of the corresponding bifurcation and display the same value on the x axis. **B:** The antipodal points described for A are projected onto a single sphere that stands for A's spheres cast in a concentric way so that the center is the same for all of them.

Theorem

Re-BUT. If $f:2^{Sn} \rightarrow R^n$ is a continuous function, then $f(\text{Re}1) = f(\text{Re}2)$ for a pair of regions Re1, Re2 on 2^{Sn} (Peters, 2016).

Proof. Given Re1 in 2^{Sn}, we know that there are many possible regions Re2 with matching feature values. The value of $f(\text{Re}1)$ is a feature value of region Re1. From the fact that there is at least one other region Re2 descriptively the same as Re1 in 2^{Sn}, we have $f(\text{Re}1) = f(\text{Re}2)$.

Example. Let $f(\text{Re}1)$ equal the area of Re1 on an n-sphere. Because there are many regions of an n-sphere with area the same as Re1, let Re2 be one of those regions. Then, $f(\text{Re}1) = f(\text{Re}2)$ (Fig. 5). This means that the antipodal points restriction from the classical BUT is no longer required. We can also consider homotopic
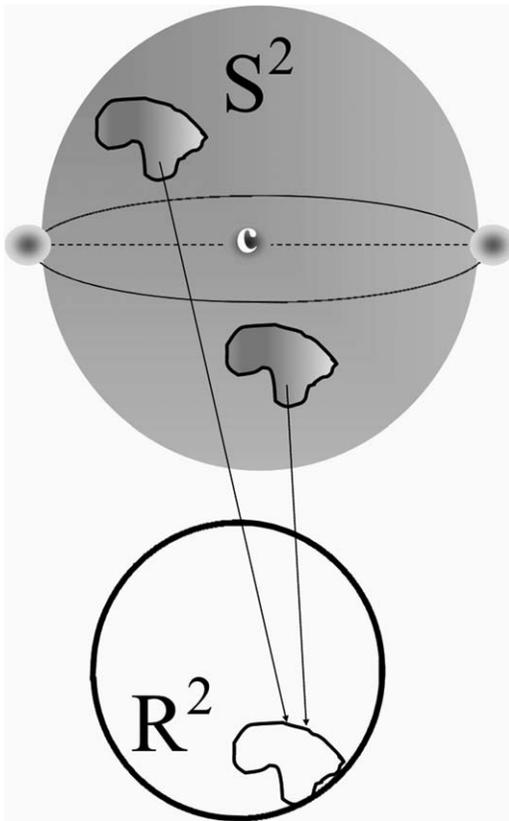
Fig. 5. Simplified sketch of the Re-BUT. The functions with matching description are not required to be antipodal. Thus, two signals, if equipped with a signal matching, may be embedded in every zone of the *n*-sphere.

brain regions on an *n*-sphere that are either adjacent or far apart, and the ReBUT applies provided that there is a pair of regions on *n*-sphere with the same feature values. We are thus allowed to say that the two points are not required to be antipodal to be described together. This makes it possible, for example, to evaluate matching signals from neuroimaging techniques, even if they are not opposite but near each other.

An Example Based on Multisensory Integration: Hierarchical Structures of the Brain

The Re-BUT applies nicely to multisensory integration (Klemen and Chambers, 2012); two environmental stimuli from different sensory modalities display similar features when mapped into cortical neurons. For example, an observer stands in front of the surrounding environment (Fig. 6), and a guitar player is embedded in the environment. The observer perceives, through his different sense organs such as his ears and eyes, the sounds and the movements produced by the player. The guitar player stands for an object embedded in a three-dimensional sphere. The two different sensory modalities produced by the player (sounds and movements) stand for nonantipodal points on the sphere's circumference. Even if objects

belonging to different regions can be either different or similar depending on the objects' features (Peters, 2016), the two nonantipodal points must share the same features. In our case, both sounds and movements come from the same object embedded in the sphere, i.e., the guitar player. The two nonantipodal points project to an $n - 1$-dimensional layer, the brain cortex where multisensory neurons lie, and converge into a single multimodal signal. According to the dictates of the Re-BUT, such a single point contains "melted" messages from the two modalities, which takes into account the features of both.

The sequential processing of information is thought to be hierarchical such that the initial, low-level inputs are transformed into representations, and integration emerges at multiple processing cortical stages (Werner and Noppeney, 2009; Van den Heuvel and Sporns, 2011). Such processes of progressive message convergence could be fruitfully studied in terms of symmetries and antipodal points that converge toward a single manifold (Fig. 6). The observable brain anatomy would reside in the *n*-dimensional space (antipodal points are not glued), but, if we apply the BUT, we could hypothesize that there exists, at a certain level of abstraction, a functional space in which these homotopic regions are mapped as one single point/region, which could, for instance, make transparent the resilient redundancy of the homotopic regions at the relevant level of processing.

GENERALIZATION OF THE BUT TO SYMMETRIES OCCURRING ON HYPERBOLIC MANIFOLDS

The original formulation of the BUT describes the presence of antipodal points on spatial manifolds in every dimension, provided that the *n*-sphere is a convex, positive-curvature manifold. However, many symmetry breakings described in physics and biology (and, in particular, in the brain!) occur on manifolds equipped with another type of geometry, the hyperbolic one. The latter encloses complete Riemannian *n*-manifolds of constant sectional curvature −1 and concave shape. The models of hyperbolic space (i.e., the Klein model) share the same geometry in the sense that any of them can be related to others by a transformation that preserves the geometrical properties of the space, including isometry, though not with respect to the metric of a Euclidean embedding. From differential geometric treatments of probability measures, it is easy to see that brain manifolds traced out by sufficient statistics of a probability measure are negatively curved in nature (Watanabe et al., 2014) and therefore endowed with a hyperbolic geometry. Hyperbolic manifolds allow the study of energy gradients in brain energetic landscapes because they describe the descent to the lower energetic basins. For example, the proteins' final folded conformation is dictated by the minimum frustration principle on long time scales; proteins' energy decreases more than expected from thermodynamic claims because they assume conformations progressively more similar to the native state (Bryngelson and Wolynes,
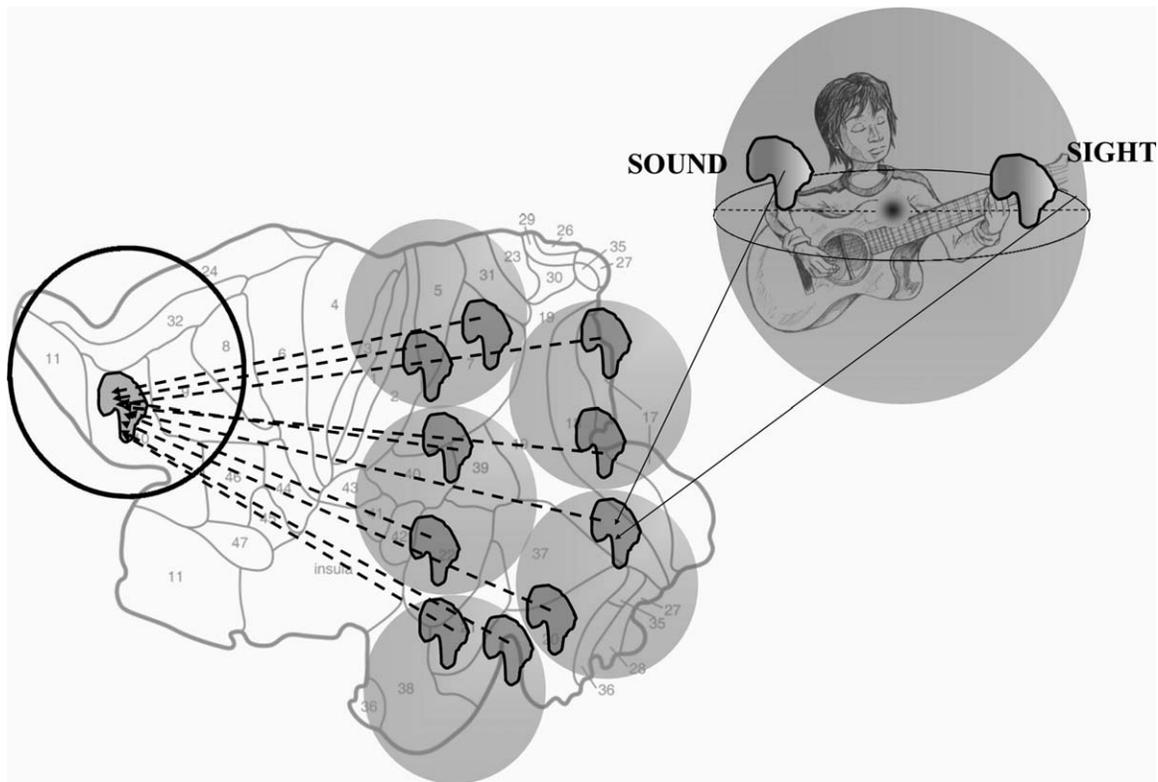
Fig. 6. Convergence of *n*-spheres' antipodal points with the same matching description. Cerebral hemispheres were unfolded and flattened into a two-dimensional reconstruction by computerized procedures (Van Essen, 2005). The final, pure abstractions achieved in the frontal lobes encompass countless different matching points from different, closely packed *n*-spheres coming from the sensory areas. The ideas (abstractions) link together antipodal points embedded in different *n*-spheres. Their projections to the "higher" areas give rise to the abstract concepts. See article text for further details.

1987; Sutto et al., 2007; Flå and Ahmed, 2011). Now the question is whether the antipodal points predicted by the BUT can be detected not only on positive-curvature manifolds, as stated by Borsuk, but also on manifolds equipped with negative curvature. In other words, is it possible to transport the BUT's antipodal points onto Riemannian manifolds with negative curvature? The answer is positive, if we perform a parallel transport of the two antipodal points of S^n onto the hyperbolic manifold (Hairer et al., 2004; Mitroi–Symeonidis, 2015). There are different routes one can take to achieve the goal. We must resort to one of the following generic transport procedures, Ehresmann connection (Ehresmann, 1950), Levi–Civita connection (Boothby, 1986), or Laplace-Beltrami operator (Jost, 2002). Also, we can retain a first-order approximation and formulate descent directions that are orthogonal to the previous descent ones through numerical analysis with the conjugate gradient–descent algorithm (Snyman, 2005). Routinely used in optimization, conjugate gradient–descent methods have been used in neuroimaging for gradient descent on manifolds traced out by energy functions (Sengupta et al., 2014). After a connection has been performed and the vectors corresponding to the antipodal points have been achieved on the hyperbolic manifold M^n, the standard projection method (Hairer et al., 2004) allows us to use the Riemann exponential map $\exp(\omega)$ to map the vector from $S^n \rightarrow M^n$ and the logarithmic map $\log(\omega)$ for the opposite mapping $M^n \rightarrow S^n$. Having achieved the center of the hyperbolic manifold M^n through the "ham-sandwich" theorem, we are allowed to map the two antipodal points from S^n to M^n and vice versa (Peters, 2016).

In summary, the BUT can also be generalized to symmetries occurring on concave manifolds. We are thus allowed to look for antipodal points and hidden symmetries on structures equipped with a negative curvature because this occurs for most brain symmetries and nervous energy landscapes.

LOOKING FOR SYMMETRIES IN THE BRAIN

The search for symmetry in the CNS is not an easy task; because of our lack of knowledge of brain function, we do not know exactly what (and where) the hidden symmetries are. Furthermore, it is unrealistic to think of obtaining in biology the mathematical accuracy of a physics experiment; i.e., although a physics experiment isolates the object of study and excludes the surrounding confounding features, a biological trial must take into account countless hidden variables. As a matter of fact, recent studies have suggested that cognitive functions do

not depend solely on electrical pulses but also on intra- and extraneuronal causes, involving supramolecular interactions among biologically active macromolecules (Tozzi, 2015). Thus, the overwhelming complexity of the factors involved is beyond our current computational comprehension. It is also important to warn that descriptions cannot unambiguously characterize the etiology of fluctuation assets because similar symmetric properties may stem from qualitatively different generators that may be difficult to distinguish with our finite amount of data (Papo, 2014).

Power Laws

It has been demonstrated that the frequency spectrum of cerebral activity exhibits a scale-invariant behavior $S(f) = 1/f^n$, where $S(f)$ is the power spectrum, f is the frequency, and n is the power spectral density, the so-called dimension of the fractal (that equals the negative slope of the line in a log power vs. log frequency scatterplot; Pritchard, 1992; Milstein et al., 2009). The brain generates fluctuations with complex scaling properties even in the absence of exogenous perturbations or changes in parameters controlling its activity (Papo, 2014), and the scale-invariant behavior involves not only the cortical electrical activity but also spontaneous neurotransmitter release (Fox and Raichle, 2007). Indeed, studies have suggested that a universal scaling is a spatiotemporal property of the brain, characterizing a large class of cerebral models and physiological signals (De Arcangelis et al., 2006). The emergence of power-law distributions has been interpreted in terms of self-organized criticality (Lübeck, 2004), a successful framework that refers to a mechanism of slow energy accumulation and fast energy redistribution, driving the system toward a critical state (De Arcangelis and Herrmann, 2010). In analyzing the scaling properties, it has been proposed that cognitive processes can be framed in terms of complex generic properties of brain activity at rest and, ultimately, of functional equations, limiting distributions, symmetries, and possibly universality classes characterizing them (Sengupta and Stemmler, 2014). Power-law distributions contain information on how large-scale physiological and pathological outcomes arise from the interactions of many small-scale processes (Jirsa et al., 2014). The above-mentioned fractal dimension gives rise to a dimension greater than the classical one dimension, which is generally attributed to the normal curves embedded in a standard Euclidean space (Mandelbrot, 1967). More importantly, the fractal dimension encourages us to take another look at the mechanisms that give rise to the brain's power-law distributions. As stated above, the BUT variants can be used for the description of antipodal points on d-spheres equipped with Hausdorff (fractal) dimension d. It is thus suitable to make use of rational numbers, instead of integer ones, as n exponents in S^n. The mechanism of a slope corresponding both to the α exponent and the n-dimension is valid both for spatial fractals (Fig. 7A) and for temporal power-laws plots (Fig. 7B).

Equalizing Excitation–Inhibition Ratios Across Cortical Neurons

Another symmetry has recently been found in the CNS. An unexpected degree of order has been revealed in the spatial distribution of synaptic strengths. This is a mechanism by which the neurons equalize the strengths of excitation (E) and inhibition (I), and the brain maintains its internal balance not only in time but also in space (Xue et al., 2014). Specifically, there is a constant E/I ratio between the total amount of excitatory and inhibitory stimulation (Sengupta et al., 2013a; Sengupta and Stemmler, 2014). E/I ratio is stable, both in vitro and in the intact and spontaneously active cerebral cortex, not only for individual pyramidal neurons at a given time (Haider et al., 2006) but also across multiple cortical neurons (Xue et al., 2014) and during neural avalanches (Lombardi et al., 2012). E and I are always matched; an optimal E/I ratio across neurons is maintained, despite fluctuating cortical activity levels, through the appropriate strengthening or weakening of inhibitory synapses, carried out by an increased recruitment of parvalbumin-expressing inhibitory neurons (Xue et al., 2014). The relationship between the two opposing forces in the mammalian cerebral cortex affects many cortical functions, such as feature selectivity and gain (Sengupta et al., 2013a) or memory of past activity (Lombardi et al., 2012). It may allow for rapid transitions between relatively stable network states (Sengupta et al., 2013b), permitting the modulation of neuronal responsiveness in a behaviorally relevant manner. E/I ratio could be interpreted as evidence of a homeostatic mechanism among strengthening and weakening processes in the adaptation of real synapses, both at the single neuron level and at the network excitability level. Homeostatic systems induce a distinction between inhibitory and excitatory connections that could contribute to symmetry breaking, leading to directed coupling and information transfer (Tognoli and Kelso, 2014). E/I ratio could thus be regarded as the symmetry of the intact and spontaneously active cerebral cortex.

A Matter of Energy?

An issue of central importance in this context is the recently proposed free-energy principle for adaptive systems, which tries to provide a unified account of action, perception, and learning (Friston, 2010). Any self-organizing system at equilibrium with its environment must minimize its (variational) free energy, thus resisting a natural tendency to disorder/entropy. The Bayesian probability of sensory states (interoceptive and exteroceptive) must have low entropy, and, because entropy is also the average self-information or "surprise," the brain must avoid surprises. The feasibility of a calculation based on entropy has been demonstrated to be useful in the basic understanding of neural function (Friston, 2008). The
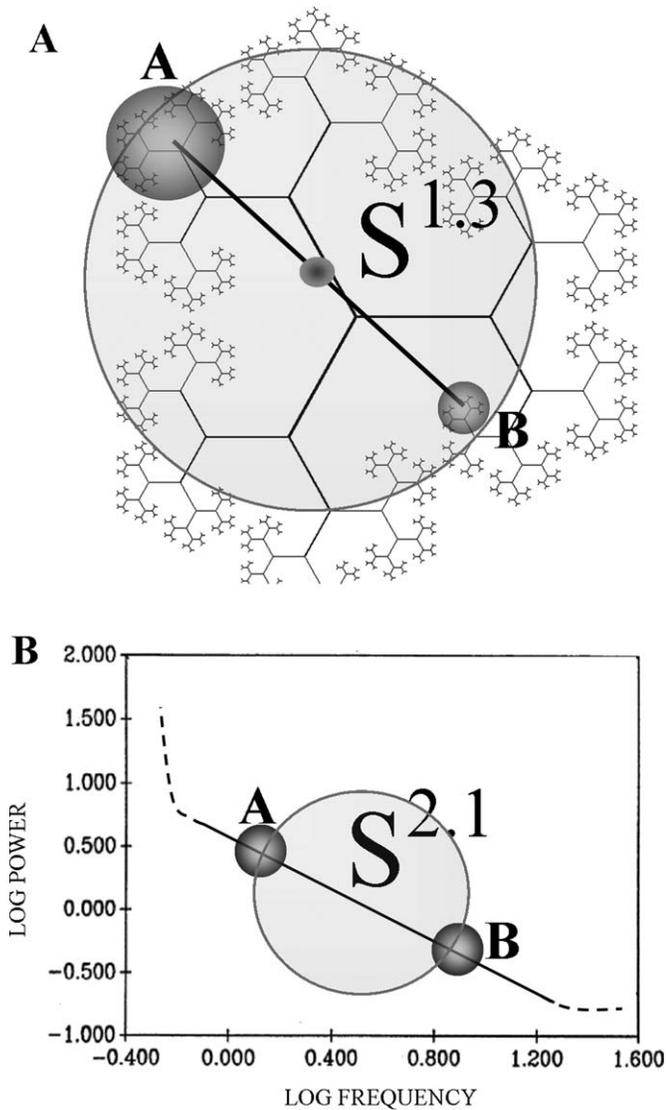
Fig. 7. Antipodal points on self-similar structures. **A:** Spatial fractals embedded in an n-sphere equipped with n corresponding to a rational number (in this case, 1.3). The circles labeled A and B depict fractals at lower and higher magnification, respectively. They have matching descriptions. **B:** The plot displays log power vs. log frequency of an electric wave along with the regression line (modified from Pritchard, 1992). The regression line's slope (in this case, $\alpha = 2.1$) is the linear alignment of the data points reflecting the dominant power law. The plot displays an example of the "temporal" variant of scale-free behavior (the so-called power laws) in the framework of the BUT; if we take into account a system with, i.e., a fractal dimension $D = 2.1$, we may regard the spatial $1/f^{\alpha}$ structure (equipped with antipodal points A and B) as embedded in a sphere $S^{2.1}$, which is equipped with a value of n corresponding to the fractal dimension α. Note that the BUT is not valid at the slope's tails, where the α exponent is lost (dotted lines at right and left of the main slope).

Fig. 8. The "oscillating" R^{n} manifold. The inputs (the environment) and outputs (in this case, the statement correlated with the environmental input) are located on two spatial n-spheres, each one equipped with antipodal points corresponding to 1 (on state) and 0 (off state) and with a center corresponding to 0.5 (fuzzy, uncertain state). The two antipodal points map to a point located on the diameter of a Euclidean manifold R^{n} that, in this case, stands for groups of neurons equipped with logic gates (prepared through another type of tessellation, the Voronoi). An input 1 is projected to R^{n} and then maps, for the Re-BUT theorem, to the output n-sphere in position 1. However, when the output (say, 0.3) is different from the input (say, 1), this means that the R^{n} sphere has moved horizontally and its center has moved. In this case, the input 1 does not map any longer to 1 on R^{n} but rather to 0.3 so that R^{n} projects to the output 0.3 even if the input is 1. If the input and the output are known (e.g., 1 and 0.3, respectively), we can calculate the change occurring in the R^{n} projection. To compare the two different projections on R^{n}, we are required to know only how much the center of the R^{n} sphere has moved. We can thus predict, given a known input, which cortical areas were activated when the output has changed; we are required to look at only the R^{n} tessellation and to see where the novel position of the point (corresponding to an activated zone) is located.

variational free-energy principle separates the environment (the external states) from the agent (the internal states; Friston, 2013). Agents can suppress free energy (or surprise) by cha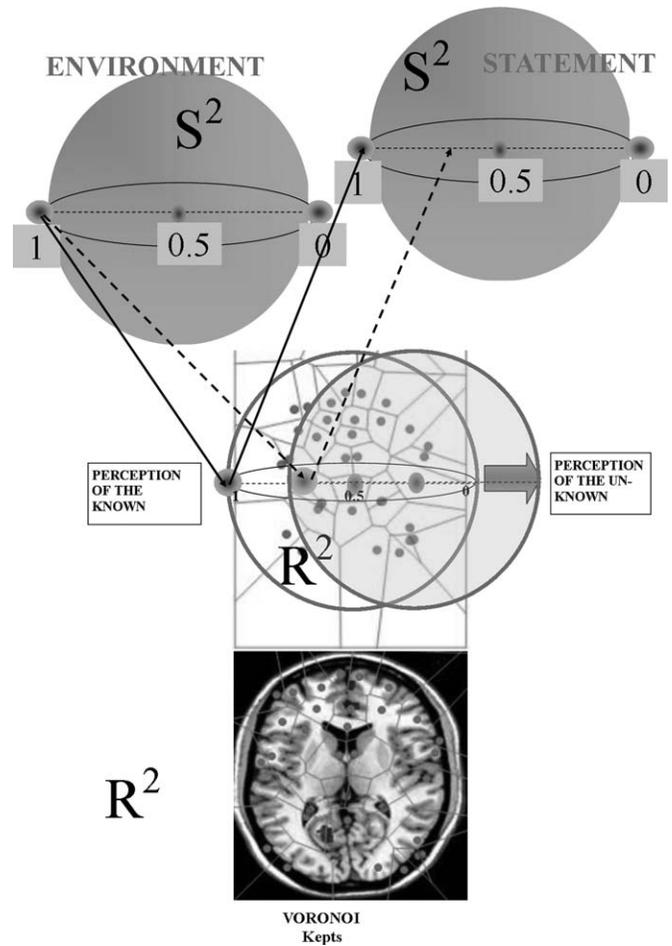nging the two things on which it depends; they can either change sensory input by acting on the world or modify their internal states via different perceptions (Sengupta et al., 2013b). Figure 8 displays the process of perception in Bayesian and topological terms. The

brain uses Bayesian beliefs to evaluate whether a matching description takes place. If it occurs, we achieve the "known" (i.e., "I see a cat"). When the description is, instead, not matching, a Kullback-Leibler divergence takes place and we attain the "unknown" (i.e., "I'm not sure whether I'm seeing a cat or a lynx"). There are two possible ways to compensate and achieve once again the known; either the R^n sphere moves, say, to the right (change in mental priors) or it moves to the left (body movements in search of the expected signals in the environment). Variations can thus be removed either through peripheral action (practical behavior) or through brain action (theoretical behavior).

The "ancient" Richard Avenarius (1907) and Ernst Mach (1897) indicated that the relation of the "I" (the corporeal presence of the human being) to the environment (the spatial presence of the object) is determined in such a way that both are present as common and inseparable elements. The "I" is found to be present just as much as the environment. This interconnection and inseparability of the "I" and its surroundings constitutes an essential association and homogeneity of the two coordinated values, setting in motion a circular process, from any point within which the whole complex of changes may start. In sum, the ideal point of rest, about which the life of the organism moves in constant oscillations, also has a logical–mathematical significance when framed as a topological theory.

The viability of the CNS is influenced by a balance between the metabolic cost incurred (in terms of ATP) by its operation and the information theoretic benefits realized by energy expenditure (Sengupta and Stemmler, 2014). The metabolic activity of the brain is remarkably constant over time (Raichle and Gusnard, 2002), and the energy budget (that is, the energy use by various neuronal processes) has been calculated (Sengupta et al., 2010). Minimizing variational free energy requires a metabolically efficient encoding that is consistent with the principles of minimum redundancy and maximum information transfer (Sengupta et al., 2013b). Maximizing mutual information and minimizing metabolic costs are two sides of the same coin; by decomposing variational free energy into accuracy and complexity, one can derive the principle of maximum mutual information as a special case of maximizing accuracy, whereas minimizing complexity translates into minimizing metabolic costs. Despite an apparent resistance to the natural tendency to increase entropy, nonequilibrium steady state is maintained (Sengupta and Stemmler, 2014). To solve this problem, one uses a (Bayesian) information theoretic construct called "variational free energy," which is a proxy for entropy; minimizing entropy production corresponds to the principle of minimizing variational free energy at each point in time. Variational free energy may be considered a sort of symmetry for systems that attain nonequilibrium steady state; accordingly, we can treat it exactly as a Lagrangian and, implicitly, as a way of minimizing entropy. Thus, the variational free energy is the Lagrangian, which is the expression of the underlying brain symmetry.

Quantum Mind Theories

Thus far, symmetrical theories of the CNS have been proposed in the framework of quantum mind theories (Freeman and Vitiello, 2008). Some of these models resemble lattice gauge theory of high-energy physics, whereas others are quantum systems, not in the sense that they consist of quantum components (such as any physical system) but that their macroscopic properties cannot be explained without recourse to an underlying quantum dynamics. Because it is not possible to test these hypotheses because of our lack of knowledge of the quantum effects in the brain, we will not go through these theories but will briefly summarize the most interesting concepts. Many models are based on the notion of spontaneous breakdown of symmetry (Freeman and Vitiello, 2008). The dynamic symmetry that gets broken is the rotational symmetry of the electric dipole vibrational field of the water molecules and other biomolecules present in the brain structures. The external input or stimulus acts on the brain as a trigger for the breakdown of the dipole rotational symmetry. When the system is not in the least-energy state, mathematical consistency requires the existence of massless particles, the Nambu-Goldstone quanta, that are normally observed in solid-state physics. It has been hypothesized that long-range correlations established by the coherent condensation of bosons may have a role in memory storage, learning, and consciousness (Matsui, 2001).

CONCLUSIONS: WHY?

This Review describes a general topological mechanism that explains the phenomenon of broken symmetries in the brain. The model is cast in an experimental fashion that has the potential of being operationalized. The question here is: why? What does a topologic reformulation help in the evaluation of brain hidden symmetries? First of all, it must be emphasized that the symmetries are widespread at every level of organization and may be regarded as the most general feature of systems, perhaps more general than free-energy and entropy constraints. Indeed, recent data suggest that thermodynamic requirements have close relationships with symmetries. The novel, interesting observation that entropy production is strictly correlated with symmetry breaking in quasistatic processes paves the way for using system invariances for estimation of the brain metastable states' free energy and the energy requirements of neural computations and information processing (Roldán et al., 2014). Thus, providing insights into symmetries provides a very general approach to every kind of brain function and dynamics. A shift in conceptualizations is evident in a brain theory of broken symmetries based on a BUT approach; the symmetries in this framework are hidden in a dimension and restored in a dimension higher and vice versa. For example, beyond the critical value, the "death" of complexity occurs, and the system falls into a supercritical regime or regularity (Zare and Gringolini, 2013). In such a vein, the fractal dimension characterizing the low-frequency spikes

of the spontaneous brain activity is lost when high-frequency spikes are activated by sensations and perceptions (Allegrini et al., 2009; Buszaki and Watson, 2012).

Furthermore, the invaluable opportunity to treat the elusive brain phenomena as topological structures allows us to describe symmetries in the language of powerful analytical tools, such as combinatorics, hereditary set systems (Matoušek, 2003), simplicial complexes, homology theory, and functional analysis. Also, generalizations of the BUT, such as the Grassmann manifolds (Dol'nikov, 1992) and the Bourgin-Yang-type theorems (Yang, 1954), could be fruitfully used in the study of nervous hidden symmetries. Embracing the BUT approach to symmetries means that the "real" brain activities can be described as paths or trajectories on abstract structures (called "topological manifolds"). This takes us into the powerful realm of algebraic topology, in which the abstract metric space (a projection of the environment's real geometric space) constitutes sufficient statistics. Moreover, attempts are being made to provide a systematic way of characterizing symmetries in the network structures of the connectome by inspecting the eigenvalues of different types of connectivity matrices (Esposito et al., 2014).

We conclude with a semantic consideration; the terms "symmetry" and "symmetry breaking" might appear somewhat arbitrary because it could be argued that the $n - 1$ space is more symmetrical than the n-dimensional space that it maps (in terms of group theory/theoretical physics), given that the antipodal gluing does not lead to opposite infinities/limits but only to a circular continuum that erases a discontinuity. We want to anticipate such possible hermeneutical confusion in some of the readership by emphasizing that our use of symmetries displays the invaluable advantage not only in treating the characteristic occurrence in cortical dynamics of complex fluctuations as a physical object (Tononi, 2008) but also in classifying measurable cognitive functions as operators acting on symmetries (Papo, 2014). By changing physical space into the dialectics symmetry/topology, paradoxes of nervous activity are more easily exposed; the BUT language opens up a virtual window into spaces beyond our brain's physical three-dimensional structure.

CONFLICT OF INTEREST STATEMENT

The authors do not have any known or potential conflicts of interest, including any financial, personal, or other relationships within three years of beginning the submitted work, with people or organizations that could inappropriately influence or be perceived to influence their work. No conflicts have been identified.

ROLE OF AUTHORS

Both authors had full access to all the data in the study and take responsibility for the integrity of the data and the accuracy of the data analysis. Study concept and design: AT, JFP. Acquisition of data: AT, JFP. Analysis and interpretation of data: AT, JFP. Drafting of the manuscript: AT, JFP.

Critical revision of the article for important intellectual content: AT, JFP. Statistical analysis: AT, JFP. Obtained funding: AT, JFP. Administrative, technical, and material support: AT, JFP. Study supervision: AT, JFP.

REFERENCES

Afraimovich V, Tristan I, Varona P, Rabinovich M. 2013. Transient dynamics in complex systems: heteroclinic sequences with multidimensional unstable manifolds. Discontinuity Nonlinearity Complexity 2:21–41.

Allegrini P, Menicucci D, Bedini R, Fronzoni L, Gemignani A, Grigolini P, West BJ, Paradisi P. 2009. Spontaneous brain activity as a source of ideal 1/f noise. Phys Rev E Stat Nonlin Soft Matter Phys 80: 061914.

Alligood KT, Sauer, Yorke YA. 1996. Chaos: an introduction to dynamical systems. In: Banchoff T, Devlin K, Gonnet GH, Marsden JE, Wagon S, editors. Textbooks in mathematical sciences. New York: Springer.

Avenarius R. 1907. Kritik Der Reinen Erfahrung von Richard Avenarius. Berlin: O.R. Reisland.

Bak P, Tang C, Wiesenfeld K. 1987. Self-organized criticality: an explanation of the 1/f noise. Phys Rev Lett 59:381–384.

Beggs JM, Timme N. 2012. Being critical of criticality in the brain. Front Physiol 3:163.

Beyer WA, Zardecki A. 2004. The early history of the ham sandwich theorem. Am Math Monthly 111:58–61.

Boothby WM. 1986. An introduction to differentiable manifolds and Riemannian geometry. New York: Academic Press.

Borsuk M. 1933. Dreisätze über die n-dimensionaleeuklidischesphäre, Fund Mathematic XX:177–190.

Borsuk M. 1958–1959. Concerning the classification of topological spaces from the standpoint of the theory of retracts. Fundamenta Mathematicae XLVI:177–190.

Borsuk M. 1969. Fundamental retracts and extensions of fundamental sequences. Fund Mathematic 64:55–85.

Borsuk M, Gmurczyk A. 1980. On homotopy types of 2-dimensional polyhedral. Fundamenta Mathematicae 109:123–142.

Bryngelson JD, Wolynes PG. 1987. Spin glasses and the statistical mechanics of protein folding. Proc Natl Acad Sci U S A 84:7524–7528.

Buzsaki G, Watson BO. 2012. Brain rhythms and neural syntax: implications for efficient coding of cognitive content and neuropsychiatric disease. Dialog Clin Neurosci 14:345–367.

Cohen MM. 1973. A course in simple homotopy theory. New York: Springer-Verlag.

Collins GP. 2004. The shapes of space. Sci Am 291:94–103.

De Arcangelis L, Herrmann HJ. 2010. Learning as a phenomenon occurring in a critical state. Proc Natl Acad Sci U S A 107:3977–3981.

De Arcangelis L, Perrone-Capano C, Herrmann HJ. 2006. Self-organized criticality model for brain plasticity. Phys Rev Lett 96:028107.

Deco G, Jirsa VK. 2012. Ongoing cortical activity at rest: criticality, multistability, and ghost attractors. J Neurosci 32:3366–3375.

Dodson CTJ, Parker PE. 1997. A user's guide to algebraic topology. Dordrecht: Kluwer.

Dol'nikov VL. 1992. A generalization of the ham sandwich theorem. Math Notes 52:771–779.

Edelsbrunner H. 2014. A short course in computational geometry and topology. Berlin: Springer.

Ehresmann C. 1950. Les connexionsinfinit'esimalesdans un espacefibrée differentiable. Bruxelles: Colloque de Topologie. p 29–55.

Esposito U, Giugliano M, van Rossum M, Vasilaki E. 2014. Measuring symmetry, asymmetry, and randomness in neural network connectivity. PloS One 9:e100805.

Flå T, Ahmed S. 2011. Evolution of cold-adapted protein sequences. In: Fung GPC, editor. Sequence and genome analysis II: methods and applications. iConcept Press.

Fox KC, Spreng RN, Ellamil M, Andrews-Hanna JR, Christoff K. 2015. The wandering brain: meta-analysis of functional neuroimaging studies of mind wandering and related spontaneous thought processes. Neuroimage 111:611–621.

Fox MD, Raichle ME. 2007. Spontaneous fluctuations in brain activity observed with functional magnetic resonance imaging. Nat Rev Neurosci 8:700–711.

Fraiman D, Chialvo DR. 2012. What kind of noise is brain noise: anomalous scaling behavior of the resting brain activity fluctuations. Front Physiol 3:307.

Frank NP, Hart SM. 2010. A dynamical system using the Voronoï tessellation. Am Math Monthly 117:92–112.

Freeman WJ, Vitiello G. 2008. Dissipation and spontaneous symmetry breaking in brain dynamics. J Phys A Math Theor 41:304042.

Friston K. 2008. Hierarchical models in the brain. PLoS Comput Biol 4: e1000211.

Friston K. 2010. The free-energy principle: a unified brain theory? Nat Rev Neurosci 11:127–138.

Friston K. 2013. Life as we know it. J R Soc Interface 10:20130475.

Friston K, Sengupta B, Auletta G. 2014. Cognitive dynamics: from attractors to active inference. Proc IEEE 102:427–445.

Haider B, Duque A, Hasenstaub AR, McCormick DA. 2006. Neocortical network activity in vivo is generated through a dynamic balance of excitation and inhibition. J Neurosci 26:4535–4545.

Hairer E, Lubich C, Wanner G. 2004. Geometric numerical integration: structure preserving algorithms for ordinary differential equations. New York: Springer.

Higgs P. 1964. Broken symmetries and the masses of gauge bosons. Phys Rev Lett 13:508–509.

Jirsa VK, Stacey WC, Quilichini PP, Ivanov AI, Bernard C. 2014. On the nature of seizure dynamics. Brain 137:2210–2230.

Jordan DW, Smith P. 2007. Nonlinear ordinary differential equations: introduction for scientists and engineers, 4th ed. Oxford: Oxford University Press.

Jost J. 2002. Riemannian geometry and geometric analysis. Berlin: Springer-Verlag.

Klemen J, Chambers CD. 2012. Current perspectives and methods in studying neural mechanisms of multisensory interactions. Neurosci Biobehav Rev 36:111–133.

Krantz SG. 2009. A guide to topology. Washington, DC: The Mathematical Association of America.

Lombardi F, Herrmann HJ, Perrone-Capano C, Plenz D, de Arcangelis L. 2012. Balance between excitation and inhibition controls the temporal organization of neuronal avalanches. Phys Rev Lett 108:228703.

Lübeck S. 2004. Universal scaling behavior of nonequilibrium phase transitions. Int J Mod Phys B 18:3977–4118.

Mach E. 1897. The analysis of sensations. Mineola, NY: Dover.

Mandelbrot B. 1967. How long is the coast of Britain? Statistical self-similarity and fractional dimension. Science 156:636–638.

Manetti M. 2015. Topology. Heidelberg: Springer.

Marsaglia G. 1972. Choosing a point from the surface of a sphere. Ann Math Statist 43:645–646.

Matoušek J. 2003. Using the Borsuk-Ulam Theorem. Lectures on topological methods in combinatorics and geometry. Berlin Heidelberg: Springer-Verlag.

Matsui T. 2001. Gauge symmetry and neural networks. In: Janke W, et al., editors. Fluctuating paths and fields. Singapore: World Scientific. p 271–280.

Milstein J, Mormann F, Fried I, Koch C. 2009. Neuronal shot noise and Brownian 1/f2 behavior in the local field potential. PloS One 4:e4338.

Mitroi-Symeonidis F-C. 2015. Convexity and sandwich theorems. Eur J Res Appl Sci 1:9–11.

Moura E, Henderson DG. 1996. Experiencing geometry: on plane and sphere. Upper Saddle River, NJ: Prentice Hall.

Papo D. 2014. Functional significance of complex fluctuations in brain activity: from resting state to cognitive neuroscience. Front Syst Neurosci 8:112.

Perkins TJ, Foxall E, Glass L, Edwards R. 2014. A scaling law for random walks on networks. Nat Commun 5:5121.

Peters JF. 2014. Topology of digital images. Visual pattern discovery in proximity spaces. Intelligent Systems Reference Library, vol 63. Berlin: Springer.

Peters JF. 2016. Computational proximity. Excursions in the topology of digital images. Intelligent Systems Reference Library. Berlin: Springer (submitted).

Pritchard WS. 1992. The brain in fractal time: 1/f-like power spectrum scaling of the human electroencephalogram. Int J Neurosci 66:119–129.

Raichle ME, Gusnard DA. 2002. Appraising the brain's energy budget. Proc Natl Acad Sci U S A 99:10237–10239.

Richardson MJ, Dale R, Marsh KL. 2014. Complex dynamical systems in social and personality psychology. In: Reis HT, Judd CM, editors. Handbook of research methods in social and personality psychology, 2nd ed. Cambridge: Cambridge University Press.

Roldán E, Martínez IA, Parrondo JMR, Petrov D. 2014. Universal features in the energetics of symmetry breaking. Nat Phys 10:457–461.

Sengupta B, Stemmler MB. 2014. Power consumption during neuronal computation. Proc IEEE 102:738–750.

Sengupta B, Stemmler M, Laughlin SB, Niven JE. 2010. Action potential energy efficiency varies among neuron types in vertebrates and invertebrates. PLoS Comput Biol 6:e1000840.

Sengupta B, Laughlin SB, Niven JE. 2013a. Balanced excitatory and inhibitory synaptic currents promote efficient coding and metabolic efficiency. PLoS Comput Biol 9:e1003263.

Sengupta B, Stemmler MB, Friston KJ. 2013b. Information and efficiency in the nervous system—a synthesis. PLoS Comput Biol 9: e1003157.

Sengupta B, Friston KJ, Penny WD. 2014. Efficient gradient computation for dynamical models. Neuroimage 98:521–527.

Smith R. 2013. Period doubling, information entropy, and estimates for Feigenbaum's constants. Int J Bifurcation Chaos 23:1350190.

Snyman JA. 2005. Practical mathematical optimization: an introduction to basic optimization theory and classical and new gradient-based algorithms. New York: Springer.

Sutto L, Latzer J, Hegler JA, Ferreiro DU, Wolynes PG. 2007. Consequences of localized frustration for the folding mechanism of the IM7 protein. Proc Natl Acad Sci U S A 104:19825–19830.

Taylor MB, Ehrenreich IM. 2014. Genetic interactions involving five or more genes contribute to a complex trait in yeast. PLoS Genet 10: e1004324.

Tognoli E, Kelso JA. 2014. Enlarging the scope: grasping brain complexity. Front Syst Neurosci 8:122.

Tononi G. 2008. Consciousness as integrated information: a provisional manifesto. Biol Bull 215:216–242.

Tozzi A. 2015. Information processing in the CNS: a supramolecular chemistry? Cogn Neurodyn 9:463–477.

Van de Ville D, Britz J, Michel CM. 2010. EEG microstate sequences in healthy humans at rest reveal scale-free dynamics. Proc Natl Acad Sci U S A 107:18179–18184.

Van den Heuvel MP, Sporns O. 2011. Rich-club organization of the human connectome. J Neurosci 31:15775–15786.

Van Essen DC. 2005. A population-average, landmark- and surface-based (PALS) atlas of human cerebral cortex. Neuroimage 28:635–666.

Watanabe T, Hirose S, Wada H, Imai Y, Machida T, Shirouzu I, Konishi S, Miyashita Y, Masuda N. 2014. Energy landscapes of resting-state brain networks. Front Neuroinform 8:12.

Weeks JR. 2002. The shape of space, 2nd ed. New York: Marcel Dekker.

Weisstein EW. 2015. Antipodal points. http://mathworld.wolfram.com/AntipodalPoints.html

Werner S, Noppeney U. 2009. Superadditive responses in superior temporal sulcus predict audiovisual benefits in object categorization. Cereb Cortex 20:1829–1842.

Weyl H. 1982. Symmetry. Princeton, NJ: Princeton University Press.

Willard S. 1970. General topology. Mineola, NY: Dover.

Xue M, Atallah BV, Scanziani M. 2014. Equalizing excitation–inhibition ratios across visual cortical neurons. Nature 511:596–600.

Yang CT. 1954. On theorems of Borsuk-Ulam, Kakutani–Yamabe-Yujob, and Dynson, I. Ann Math 60:262–282.

Zare M, Grigolini P. 2013. Criticality and avalanches in neural network. Chaos Solitons Fractals 55:80–94.

Zeidler E. 2011. Quantum field theory III: gauge theory. New York: Springer.